Simplified models for waves due to steadily moving ships and submerged bodies

Scott W. McCue, **Ravindra Pethiyagoda**, **Timothy J. Moroney**

School of Mathematical Sciences, Queensland University of Technology, Brisbane QLD 4001, Australia

1. Introduction

The distinctive V-shaped wave patterns that form behind a steadily moving ship or submerged body have been the subject of intense interest from engineers, physicists and mathematicians. Using linear potential theory, there are reasonably sophisticated approaches to incorporating the shape of the vessel, such as Michell's thin ship theory, Havelock's flat ship theory, or Hogner's slender-ship theory [10, 19]. On the other hand, certain qualitative features of ship wave patterns can be studied via simple models where a hypothetical pressure is applied to the waters surface [2, 8]. Here we draw upon this simplified approach with applied pressure distributions and make connections with models for waves due to submerged vessels. We touch on linear and nonlinear theories.

We are motivated in part by the extensive use of pressure distributions to model disturbances due to moving vessels. A very crude, but commonly used, form of the pressure is a Gaussian, which is localised and decays very quickly in all directions [2, 3, 12, 13]. A slightly more realistic approach has a pressure distribution that is positive near the bow of the ship while negative near the stern [15], or even two-point pressures (one positive and one negative) [6, 18]. These models are attractive since they are easy to use and avoid the complications of the more sophisticated approaches cited above. For the related problem of flow due to a submerged vessel, we argue in section 2 that the flow can be modelled by a pressure distribution which is a combination of a localised positive pulse together with weaker negative contributions near both the bow and the stern of the ship. Alternatively, we propose a three-point pressure model (one positive and two negative) as a means to mimic the wave pattern from a steadily moving submerged vessel.

In section 3, we also briefly consider the configuration of flow past a submerged point sink and demonstrate that it shares qualitative features of models for a vessel moving on the surface of water. Linear and nonlinear computations are provided in section 4.

2. Steady flow past a submerged point doublet

2.1. Governing equations

As a prototype model for flow due to a steadily moving submerged vessel (a submarine near the surface, say), we consider flow past a point doublet of dimensional strength κ submerged a distance L from the (undisturbed) surface. Setting the background velocity to be U, the important parameters in the problem are the dimensionless doublet strength $\mu = \kappa/(UL^3)$ and the Froude number $F = U/\sqrt{gL}$. By denoting the location of the free-surface by $z = \zeta(x, y)$, the velocity potential $\phi(x, y, z)$ satisfies Laplaces equation

$$\nabla^2\phi = 0, \qquad \text{for } z < \zeta(x, y). \tag{1}$$

subject to the boundary conditions

$$\phi_x\zeta_x + \phi_y\zeta_y = \phi_z, \qquad \text{on } z = \zeta(x, y), \tag{2}$$

$$(\phi_x^2 + \phi_y^2 + \phi_z^2) + \frac{2\zeta}{F^2} = 1, \qquad \text{on } z = \zeta(x, y), \tag{3}$$

together with the near-singular behaviour

$$\phi \sim x + \frac{\mu x}{4\pi(x^2 + y^2 + (z + 1)^2)^{3/2}}, \qquad \text{as } (x, y, z) \to (0, 0, -1). \tag{4}$$

There are also the appropriate far-field conditions that $\phi \sim x$ as $x \to -\infty$ and $z \to -\infty$.

For a weak doublet, $\mu \ll 1$, we can linearise (1)-(4) by writing $\zeta = \mu\zeta_1$,

$$\phi = x + \frac{\mu x}{4\pi(x^2 + y^2 + (z + 1)^2)^{3/2}} + \frac{\mu x}{4\pi(x^2 + y^2 + (z - 1)^2)^{3/2}} + \mu\phi_1,$$

to give

$$\nabla^2\phi_1 = 0, \qquad z < 0 \tag{5}$$

34th International Workshop on Water Waves and Floating Bodies, 7-10 April 2019, Newcastle, Australia

(a) Pressure distribution (9)   (b) Pressure distribution (12)

Figure 1: A visualisation of the pressure distributions that emulate flow past (a) a submerged doublet (9), and (b) a submerged sink (12).

$$\zeta_{1_x} = \phi_{1_z}, \quad \phi_{1_x} + \frac{\zeta_1}{F^2} + \frac{\partial}{\partial x}\left(\frac{x}{2\pi(x^2+y^2+1)^{3/2}}\right) = 0 \qquad z = 0, \tag{6}$$

together with the appropriate far-field conditions. The linear problem (5)-(6) can be solved exactly using Fourier transforms to give

$$\zeta = \frac{\mu}{2\pi^2}\int_{-\pi/2}^{\pi/2} \Re\left\{\int_0^\infty \frac{k^2 \mathrm{e}^{-k}}{k - \sec^2\psi/F^2}\mathrm{e}^{-ik(|x|\cos\psi + y\sin\psi)}\,\mathrm{d}k\right\}\mathrm{d}\psi$$
$$- \frac{H(x)\mu F^2}{\pi}\int_{-\pi/2}^{\pi/2} k_0^3\cos^2\psi \mathrm{e}^{-k}\sin(k_0(x\cos\psi + y\sin\psi))\,\mathrm{d}\psi \tag{7}$$

where the path of k-integration is taken under the pole $k = \sec^2\psi/F^2$.

We choose this problem with a submerged doublet because the linear version (1)-(4) is equivalent to flow past a submerged sphere of radius $(\mu/2\pi)^{1/3}$, which is possibly the most simple nontrivial geometry for flow past a submerged body [5]. The full nonlinear problem (1)-(4) loses this precise interpretation, as the spherical body becomes distorted as μ increases. Linear and nonlinear solutions of this problem are studied in some detail in [11].

2.2. Equivalence to flow past a pressure distribution

Now consider the problem of flow past a pressure distribution $\mu p(x, y)$ applied to the surface of the water. Here we can linearise for $\mu \ll 1$ by writing $\zeta = \mu\zeta_1$, $\phi = x + \mu\phi_1$, to give (5) with

$$\zeta_{1_x} = \phi_{1_z}, \quad \phi_{1_x} + \frac{\zeta_1}{F^2} + p(x, y) = 0 \qquad z = 0. \tag{8}$$

As mentioned in the Introduction, a typical choice for p is the Gaussian $p = \exp\left(-\pi^2(x^2+y^2)\right)$, which is a single pulse that decays equally in all directions. This pressure function is deficient in the sense that it is not motivated by a real vessel.

On the other hand, by comparing (6) with (8), we see that the choice

$$p(x, y) = \frac{\partial}{\partial x}\left(\frac{x}{2\pi(x^2+y^2+1)^{3/2}}\right) = -\frac{\partial^2}{\partial x^2}\left(\frac{1}{2\pi\sqrt{x^2+y^2+1}}\right) \tag{9}$$

produces a linearised free surface that is exactly the same as that for the problem of flow past a submerged doublet. Thus, in (9) we have a pressure distribution that can be used as a simple model for flow past a submerged body. As we can see by Figure 1(a), this pressure is made up of a large pulse centred on the origin, together with two smaller negative pulses at the front and back of the distribution. Note that the local minima of (9) are at $y = \pm\ell = \pm\sqrt{6}/2$.

2.3. Three-point pressure model

The results in section 2.2 above motivate an even simpler model which involves three point pressures:

$$p(x, y) = -\delta(0, -\ell) + 2\delta(0, 0) - \delta(0, \ell), \tag{10}$$

where $\delta(x, y)$ is the Dirac delta function. The choice of the prefactors in (10) is made so that the net force on the surface provided by (10) is zero, which is also true for (9).

Our three-point pressure model (10) for submerged bodies is the analogue of the two-point pressure version used for ship models [6, 9]. We propose that (10) can be used in studies of wave interference, for example, as undertaken by Noblesse and coworkers in their work on traditional ship waves [9, 17].

3. Steady flow past a submerged point sink

As mentioned above, a standard simple model for a vessel travelling on the surface of water is a pressure distribution which is positive near the bow and negative near the stern. It turns out that such a model is closely related to flow past a submerged point sink. To see this connection, note that the problem for flow past a submerged point source (of dimensional strength m) is (1)-(3) with the additional singular behaviour

$$\phi \sim x - \frac{\epsilon}{4\pi\sqrt{x^2+y^2+(z+1)^2}} \qquad \text{as } (x,y,z) \to (0,0,-1), \tag{11}$$

where $\epsilon = m/(UL^2)$ is the dimensionless strength of the source. Note that for flow past a submerged sink, we simply take $\epsilon < 0$.

One physical interpretation of this problem, at least for the linear regime $|\epsilon \ll 1|$, is that it is equivalent to flow past a submerged semi-infinite Rankine body with a rounded nose. The body approaches a cylinder of radius $(\epsilon/\pi)^{1/2}$ as $x \to \infty$ for a source ($\epsilon > 0$) and $x \to -\infty$ for a sink ($\epsilon < 0$) [1]. Again, this precise interpretation is altered for nonlinear flows as the shape of the body is distorted as ϵ increases. This problem is treated in some detail in [4, 7, 11, 14]. See also the recent study by Wu *et al.* [17], who consider this configuration in the context of more sophisticated submerged bodies.

The main point we wish to make here is that the linearised problem of flow past a pressure distribution $\epsilon p(x,y)$, where

$$p = -\frac{\partial}{\partial x}\left(\frac{1}{2\pi\sqrt{x^2+y^2+1}}\right), \tag{12}$$

produces a free surface that is exactly the same as that for the problem of flow past a submerged source/sink, with $\epsilon > 0$ for source and $\epsilon < 0$ for a sink. A plot of $\epsilon p(x,y)$ with (12) and $\epsilon < 0$ is provided in Figure 1(b). We see that this function captures the required qualitative features for flow due to a vessel travelling on the water's surface, namely a positive pressure near the bow and a negative pressure near the stern. Thus, we see there is a close connection between flow past a submerged sink and that due to a moving ship.

4. Nonlinear results

We now provide representative solutions for the linear and nonlinear problems summarised above in Figure 2. The exact linear solution for flow past a submerged doublet is listed in equation (7), while the linear solution for flow past a submerged sink is given in [11] (and elsewhere). For the nonlinear versions of the problems, we solve the equations numerically by reformulating them as a integro-differential equation using Green's second formula [4, 16]. By enforcing the integral equation at grid points over a two-dimensional mesh, a system of nonlinear algebraic equations is derived. A consequence of the integral nature of the governing equations is that the Jacobian for the system is dense, which provides significant computational challenges in terms of storage and factorisation. We deal with these issues by applying a Jacobian-free Newton-Krylov method together with a banded preconditioner taken from the relevant linear problems, thus avoiding the need to ever form or factorise the Jacobian. GPU acceleration is used to speed up function evaluation times (see [14] for details).

By observing the free-surface profiles in Figure 2(a) and (b) we see that the nonlinear solution for flow past a submerged doublet (part (b)) is relatively similar to the linear solution (part (a)), except that the nonlinear surface has sharper crests and divergent waves that resemble dorsal fins. The linear solution for flow past the pressure distribution (9) is the same as in part (a), as described above. The nonlinear solution, however, is not exactly the same as the nonlinear solution for flow past a submerged doublet, as we can see by comparing the surfaces in parts (b) and (c).

We can make analogous observations from glancing at Figure 2(d)-(e). Here the linear surface for flow past a submerged point sink, shown in part (d), is the same as that for linear flow past the pressure distribution (12). With nonlinearity taken into account, these two configurations provide rather different free-surface profiles, as we can see by comparing (e) and (f). On this scale it appears that the divergent waves for flow past a sink are sharper, again shaped like dorsal fins.

5. Summary

We are inspired to make connections between flows past submerged bodies and pressure distributions. By considering the prototype problem of flow past a submerged doublet (which in the linear regime is equivalent to flow past a spherical body), we show that the resulting wave pattern is exactly the same as that for the linear problem of flow past the pressure distribution (9). This type of connection is worth pursuing because flows past pressure distributions are used routinely as toy models for ship wakes, so it is of value to derive a pressure distribution that is relevant for the less well studied case of a submerged body. Note that the qualitative features of (9) (with a large positive pressure in the middle with two negative pressures near the front and back)

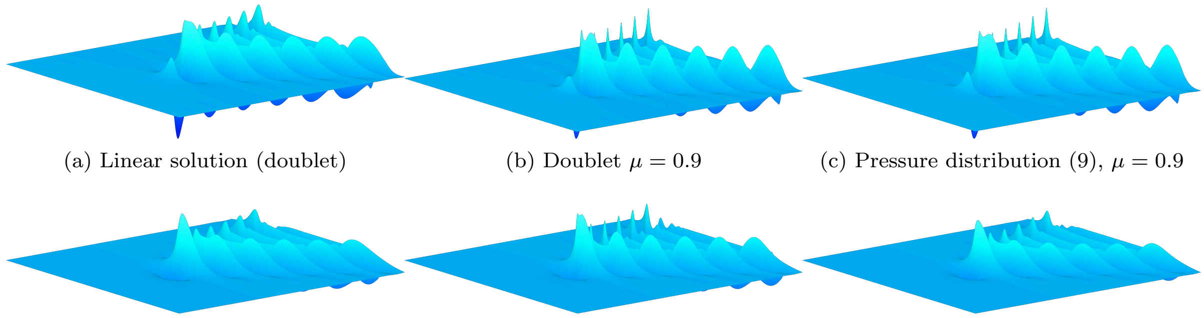

(a) Linear solution (doublet) (b) Doublet $\mu = 0.9$ (c) Pressure distribution (9), $\mu = 0.9$

(d) Linear solution (sink) (e) Sink $\epsilon = -1$ (f) Pressure distribution (12), $\epsilon = -1$

Figure 2: Free surface profiles for (a)-(c) flow past a submerged doublet and its equivalent pressure distribution (9), and (d)-(f) flow past a submerged sink and its equivalent pressure distribution (12). All solutions are for Froude number $F = 0.9$ and on a 735×237 mesh with $x_0 = -18$, and $\Delta x = \Delta y = 0.068665$.

are in contrast to that considered reasonable for a vessel travelling on the surface of water, for which a more appropriate model has a positive pressure near the bow and a negative pressure near the stern [9, 15].

In the spirit of formulating a minimalist model, we propose the three-point pressure set-up (10) (with one positive and two negative point pressures) as a simple way to mimic how waves are created behind a submerged body moving at constant speed. This approach is analogous to the two-point pressure model for ship waves widely used in the literature. It is worth pursing the three-point pressure model further by comparing and contrasting with more sophisticated models for submerged bodies.

It is interesting to note that flow past a submerged point sink (which is equivalent to flow past a submerged semi-infinite Rankine body with a rounded nose) shares qualitative features with flow due moving ship. We establish this connection by observing that the wave pattern for linear flow past a submerged point sink is equivalent to flow past the pressure distribution (12), which is qualitatively similar to the two-point pressure model used in the literature for ship wakes.

Finally, we show that while certain different flow configurations provide the same wave patterns in the linear regime, the precise equivalence does not carry over in the fully nonlinear case. Further, we see that nonlinear solutions exhibit interesting properties such as steep waves with sharp crests that are not observed in their linear counterparts. There are a number of open problems in the mathematical study of steady nonlinear ship waves, such as determining the form of the steepest divergent wave possible.

Funding: This work is supported by the Australian Research Council via DP180103260.

References

[1] G. K. Batchelor. *An Introduction to Fluid Dynamics.* Cambridge University Press, 1967.

[2] A. Darmon, M. Benzaquen, and E. Raphaël. Kelvin wake pattern at large Froude numbers. *J. Fluid Mech.*, 738:R3, 2014.

[3] S. Å. Ellingsen. Ship waves in the presence of uniform vorticity. *J. Fluid Mech.*, 742:R2, 2014.

[4] L. K. Forbes. An algorithm for 3-dimensional free-surface problems in hydrodynamics. *J. Comput. Phys.*, 82:330–347, 1989.

[5] H. Lamb. *Hydrodynamics.* Cambridge University Press, 4th ed edition, 1916.

[6] Y. Li. Wave-interference effects on far-field ship waves in the presence of a shear current. *J. Ship Res.*, 62:37–47, 2018.

[7] C. J. Lustri and S. J. Chapman. Steady gravity waves due to a submerged source. *J. Fluid Mech.*, 732:660–686, 2013.

[8] S. Miao and Y. Liu. Wave pattern in the wake of an arbitrary moving surface pressure disturbance. *Phys. Fluids*, 27:122102, 2015.

[9] F. Noblesse, J. He, Y. Zhu, L. Hong, C. Zhang, R. Zhu, and C. Yang. Why can ship wakes appear narrower than Kelvin's angle? *Euro. J. Mech. B/Fluids*, 46:164–171, 2014.

[10] F. Noblesse, F. Huang, and C. Yang. The Neumann-Michell theory of ship waves. *J. Eng. Math.*, 79:51–71, 2013.

[11] R. Pethiyagoda, S. W. McCue, and T. J. Moroney. What is the apparent angle of a Kelvin ship wave pattern? *J. Fluid Mech.*, 758:468–485, 2014.

[12] R. Pethiyagoda, S. W. McCue, and T. J. Moroney. Wake angle for surface gravity waves on a finite depth fluid. *Phys. Fluids*, 27:061701, 2015.

[13] R. Pethiyagoda, S. W. McCue, and T. J. Moroney. Spectrograms of ship wakes: identifying linear and nonlinear wave signals. *J. Fluid Mech.*, 811:189–209, 2017.

[14] R. Pethiyagoda, S. W. McCue, T. J. Moroney, and J. M. Back. Jacobian-free Newton-Krylov methods with GPU acceleration for computing nonlinear ship wave patterns. *J. Comput. Phys.*, 269:297–313, 2014.

[15] R. Pethiyagoda, T. J. Moroney, G. J. Macfarlane, J. R. Binns, and S. W. McCue. Time-frequency analysis of ship wave patterns in shallow water: modelling and experiments. *Ocean Engng*, 158:123–131, 2018.

[16] E. Părău and J.-M. Vanden-Broeck. Nonlinear two- and three-dimensional free surface flows due to moving disturbances. *Euro. J. Mech. B/Fluids*, 21:643–656, 2002.

[17] H. Wu, J. He, H. Liang, and F. Noblesse. Influence of Froude number and submergence depth on wave patterns. *Euro. J. Mech. B/Fluids*, in press, 2018.

[18] Y. Zhu, J. He, H. Wu, W. Li, F. Noblesse, and G. Delhommeau. Elementary ship models and farfield waves. *Euro. J. Mech. B/Fluids*, 67:231–241, 2018.

[19] Y. Zhu, H. Wu, C. Ma, J. He, W. Li, D. Wan, and F. Noblesse. Michell and Hogner models of far-field ship waves. *Appl. Ocean Res.*, 68:194–203, 2017.